Table 1 Comparison of the Expression Status of Genes in Microarrays Between aRNA Samples Prepared from UFT and Methacarn-Fixed PET[a]

Tissue Status	UFT		Methacarn-Fixed PET
aRNA Sample	1× amplified	2× amplified	2× amplified
Rates with gene probes for each expression status (%)			
Present	40.3	36.9	36.4
Absent	57.5	60.9	61.5
Marginal	2.2	2.2	2.1
Signal ratio with the GAPDH gene (3′/5′, × fold)	1.1	12.3	11.3

aRNA, antisense RNA; UFT, unfixed frozen tissue; PET, paraffin-embedded tissue; GAPDH, glyceraldehyde-3-phosphate dehydrogenase.
[a]Liver tissue of a rat treated daily with sodium phenobarbital (80 mg/kg body weight, s.c.) for three days was used.

ies) serum, sections were incubated with primary antibodies, overnight at 4°C, and subsequently with biotinylated secondary antibody for 60 min at room temperature. All antibodies used were diluted with 0.5% casein in PBS before application. Immunodetection was carried out with the horseradish peroxidase–avidin–biotin complex utilizing a VECTASTAIN™ Elite ABC kit (Vector Laboratories, Burlingame, CA), with 3,3′-diaminobenzidine/H_2O_2 as the chromogen. Sections were counterstained with hematoxylin for microscopic examination. For quantitative measurement of the numbers of nuclei immunoreactive for PARP, bilateral portions of a 250 × 250 μm area covering the SDN region were subjected to analysis under 200× magnification. Also, nuclei immunoreactive for MT-1/2 were counted in bilateral MPOAs by randomly selecting three fields (125 × 125 μm area) on each side under 400× magnification. For each antigen (PARP and MT-1/2), mean ratios of nuclear immunoreactive cells to the total cells counted in each side were estimated.

Data Analysis

Scanned output files of microarrays were visually inspected for hybridization artifacts, and then expression signals for each gene were measured by calculating pixel intensities using a Microarray Suite software package (Version 5.0, Affymetrix). With this software, the expression status of each gene, whether present, absent, or marginally expressed, was judged. Exclusion of genes showing absence in at least three of six samples of the two groups for comparison of expression, normalization of expression data, and statistical comparisons were performed using GeneSpring™ software (Version 5; Silicon Genetics; Redwood City, CA). For microarray data in the validation study of expression fidelity with methacarn-fixed PET specimens, per chip normalization was performed by dividing the signal strength for each gene with the level of the 50th percentile of the measurement in the chip, and per gene normalization with average signal strength of the identical gene of three 1×-amplified aRNAs samples from UFTs. With regard to the microarray data for microdissected MPOA, per chip normalization was performed by dividing the signal strength of each gene by the level of the spike RNA signal in each sample, and per gene normalization with average signal strength of the identical gene in three untreated control samples. Average relative expression values were determined for each gene in the treatment group, and genes showing expression changes with ≥2-fold differences were first estimated. Then, comparison of expression data between the untreated controls and each treatment group was performed using Student's *t*-test with multiple testing corrections applying Benjamini and Hochberg false positive discovery rate calculations, and genes showing statistical significance with a p value <0.05 were selected.

To assess fidelity of expression patterns in microarrays between the 2×-amplified aRNA samples from methacarn-fixed liver PETs and 1×- and 2×-amplified samples from liver UFTs, Pearson's correlation coefficients (r) for each combination were estimated using all genes included in the array.

For the real-time RT-PCR data, expression values were normalized to the amplification efficiency of the first-round *in vitro* transcription by dividing the expression values with the signal level of spike RNA included in each sample. Differences in expression levels between sexes were analyzed by the Student's *t*-test, when the variance proved to be homogeneous among groups using the test for equal variance. If a significant difference in the variance was observed, a Welch's *t*-test was performed.

Morphometrically analyzed data for nuclear immunoreactive cell ratios of PARP and MT-1/2 were compared by Student's and Welch's *t*-tests. Regarding immunoreactivities on which morphometric analysis could not be applied, total incidence of immunoreactive cases and grades of intensity were visually analyzed and statistically compared using the Fisher's exact probability test and Mann–Whitney's *U*-test, respectively.

RESULTS

Expression Fidelity in Methacarn-fixed PETs

Expression fidelity of the microdissected small tissue samples in microarray analysis might be influenced by tissue processing for microdissection and/or multiround amplification. To clarify the effect of tissue processing for microdissection (methacarn-fixation and following paraffin-embedding) on the expression

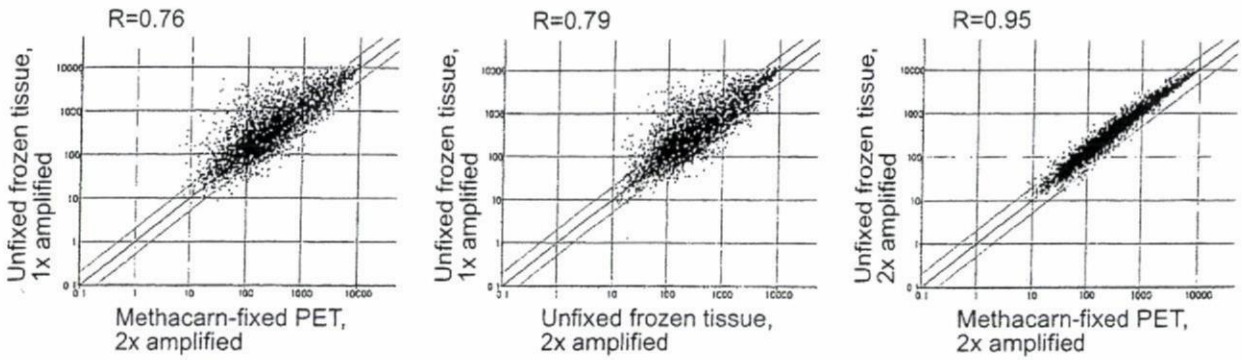

Figure 2 Scatter plot analysis of gene expression profiles of aRNA samples derived from methacarn-fixed PET and UFT of rat liver.

fidelity after 2×-amplification, expression in the second-round amplified aRNA samples was compared with that obtained from the 1×- or 2×-amplified aRNAs from UFT. With the 8799 probes included in the array used, percentages of expression status (present, absent, and marginal) were similar among aRNA-preparations irrespective of the tissue status and the amplification cycle (Table 1). However, preferential amplification of the 3′ portions was evident with 2× amplification in both UFT and methacarn-fixed PET cases (Table 1). By scatter plot analysis, high correlations were observed in the expression profiles between the 2×-amplified aRNAs from methacarn-fixed PET and UFT ($r = 0.95$, $n = 3$; Fig. 2). When the correlation of gene expression levels was examined between the 1×-amplified aRNAs from UFT and 2×-amplified ones from either methacarn-fixed PET or UFT, r values were similar, but relatively low when compared with the value for the correlation between the two 2× amplified examples, indicating a lowered expression fidelity in the methacarn-fixed PET because of the second-round amplification. When the number of genes showing presence was examined for 2×-amplified methacarn-fixed PET and 1×-amplified UFT aRNAs, 3173 probes were positive in common (as shown in Fig. 3). The numbers of probes showing presence solely in the methacarn-fixed PET (2× amplified) and UFT (1× amplified) were 373 and 822, respectively, suggesting that 10.5% of the total genes exhibiting presence in the 2×-amplified samples should be regarded to be false positive, and that 20.6% of the present genes in the 1×-amplified samples from UFT lost their signals after two-round amplification. It is possible that the distance from the poly(A) tail to the positions of the probes may affect the expression status of each gene after the second-round *in vitro* transcription due to preferential amplification of the 3′-terminal portion. Among genes showing presence solely in the methacarn-fixed PET (2× amplified) and UFT (1× amplified), sequence information including the full 3′-untranslated region from the poly(A) tail was available for six and five genes, respectively. The mean distances from the 5′-end of the probes (both 5′- and 3′-most probes) to the 5′-end of poly(A) tail expressed as the number of nucleotides were examined for these (Table 2), and as expected, they were shorter with 2×-amplified aRNA samples from methacarn-fixed PET than with their 1×-amplified counterparts from UFT. These results indicate that the decline in expression fidelity with 2×-amplified samples is mainly due to preferential amplification at the 3′-portions by the second-round amplification and methacarn fixation and paraffin-embedding did not apparently affect the fidelity.

Gene Expression Profiles of MPOA of Neonates Acutely Treated with EB or FA

In the MPOAs at PND 2, about 3600 genes showed presence in both sexes in untreated controls. Sex dif-

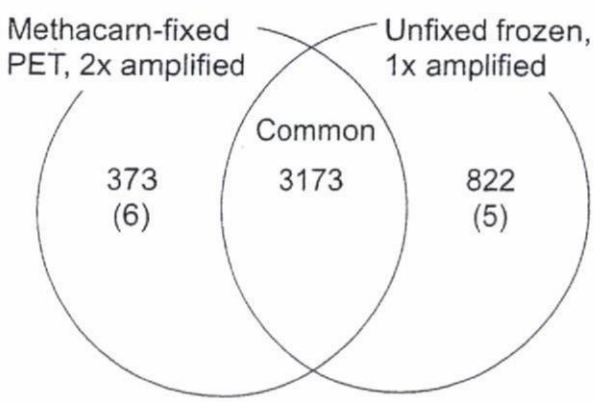

Figure 3 Gene populations showing presence with aRNA samples 2×-amplified from methacarn-fixed PET and 1×-amplified from UFT.

Table 2 Mean Distance from the Probes to the Poly(A) Tail Positions of Genes Showing Presence Solely in the UFT or Methacarn-Fixed PET[a]

aRNA Sample	UFT, 1× amplified	Methacarn-Fixed PET, 2× amplified
Mean distance from the 5′ end of the poly(A) tail (bp)		
No. of genes examined[b]	6	5
3′ end of the 5′ most probe	847	318[c]
3′ end of the 3′ most probe	569	97[c]

aRNA, antisense RNA; UFT, unfixed frozen tissue; PET, paraffin-embedded tissue.

[a] Genes obtained from microarray data in Table 1 were examined.

[b] All genes with sequence information for the 3′-untranslated region were examined.

[c] Significantly different from the unfixed frozen samples ($p < 0.01$).

ferences for male- or female-biased expression were found for 21% and 6% of all present genes, respectively (≥2-fold; Table 3). On EB-treatment, females demonstrated a greater number of genes with expression change. In males, up-regulation by EB was found for only 25 genes, all of them within 2- to 5-fold, and no genes showed down-regulation. In females, up-regulation was detected for a total of 586 genes after EB-treatment (≥2-fold), with 52 genes exhibiting ≥5-fold increase. When compared with up-regulated genes, down-regulated examples were fewer in number in females, with a total of 187 genes showing ≤1/2-fold down-regulation when compared with the vehicle control level. Among them, 33 genes showed ≤1/5-fold down-regulation when compared with vehicle controls. Relatively small numbers of genes showed altered expression on FA-treatment in both sexes. In males, only two and three genes showed up- and down-regulation, respectively (2- to 5-fold change), and in females, three and 22, all of them exhibiting 2- to 5-fold change, except for one gene with ≤1/5-fold up- and down-regulation, respectively.

Among genes showing male-biased expression (≥2-fold difference; 740 genes in total), 59% of them exhibited up-regulation on EB-treatment in females (≥2-fold; 437 genes in total), one of them also exhibiting up-regulation by FA in males (as shown in Fig. 4). One example alone showed down-regulation by FA in males. On the other hand, among genes showing female-biased expression (≥2-fold difference; 203 genes in total), 55% of them exhibited down-regulation by EB in females (≤1/2-fold; 111 genes in total). Among them, a total of 10 genes also showed altered expression by FA; nine genes down-regulated in females and one gene up-regulated in males. On the other hand, five female-predominant genes exhibited up-regulation by EB in males, four of them also showing down-regulation by EB in females, with one gene each further showing down-regulation in females and up-regulation in males by FA-treatment.

When genes that demonstrated changed expression levels in both sexes by the chemical treatments were examined, four genes encoding the LINE retrotransposable element 3, L1Rn B6 repetitive DNA element, ADP-ribosyltransferase (adprt) 1, and NonO/p54nrb homolog, exhibited up-regulation in males and down-regulation in females by EB-treatment and also female-biased expression (Table 4). Expression levels for genes showing male-biased expression were not affected by EB. FA-treatment did not alter the expression level of any gene involving both sexes.

Table 5 shows the list of genes showing altered expression in the MPOA of either sex common to both chemicals. Among the total of 15, 12 showed down-regulation in females common to EB and FA, eight of them exhibiting female-biased expression, i.e., for protein tyrosine phosphatase, receptor type, F (*PTPRF*); DAP-like kinase (*dlk*); glutamate receptor, kainate receptor subunit (KA1); dyskeratosis congenita 1 (*dyskerin*); L1Rn B6 repetitive DNA element; *MAP2*; expressed sequence tag (EST), similar to the mouse estrogen-responsive finger protein (*efp*); and glutamate receptor, ionotropic, AMPA subtype (GluR1).

Table 3 Number of Genes Showing Sex Differences in Basal Expression as well as Alteration After EB or FA Treatment in the Neonatal MPOA ($p < 0.05$)

Difference/Change (× fold)	2–5	≥5
Sex difference		
Males > females	676	64
Females > males	176	27
Altered by EB		
Males		
Up-regulated	25	0
Down-regulated	0	0
Females		
Up-regulated	534	52
Down-regulated	154	33
Altered by FA		
Males		
Up-regulated	2	0
Down-regulated	3	0
Females		
Up-regulated	3	0
Down-regulated	22	0

EB, estradiol benzoate; FA, flutamide; MPOA, medial preoptic area.

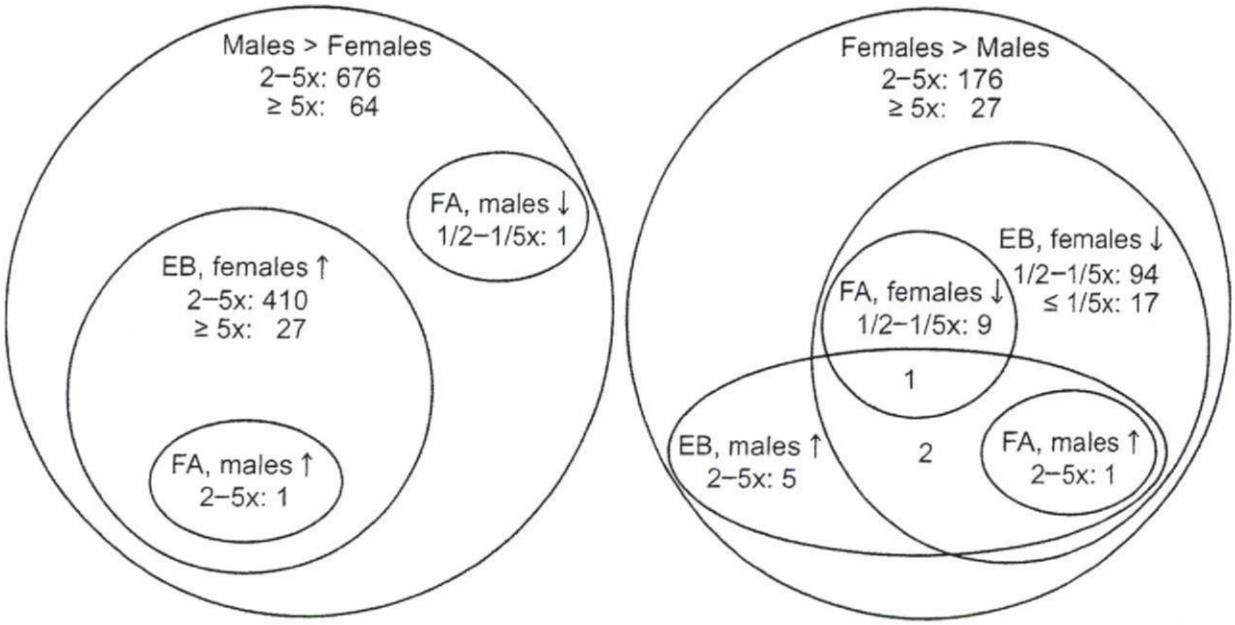

Figure 4 Distribution of gene populations showing altered expression with EB and/or FA-treatment among those showing sex differences in expression in the neonatal MPOA.

Interestingly, two subtypes of glutamate receptors, KA1 and GluR1, exhibited this particular expression pattern, the former being detected with two different probe sets (accession nos. U08257 and X59996). Without showing sex differences in the basal expression, expression of five genes were influenced by EB and FA, the following four exhibiting down-regulation in females with both chemicals: myeloid/lymphoid or mixed-lineage leukemia (trithorax (drosophila) homolog); translocated to, 3; cyclin D1; serine/threonine kinase 25; and neurotrimin. On the other hand, one EST (accession no. AI639097) showed up-regulation by EB and down-regulation by FA in females. Among the genes listed in Table 5, up-regulated examples were rather few and the magnitude of up-regulation was within 2- to 3-fold. In addition to the altered expression involving both sexes after EB treatment (see above), two genes showed altered expression with FA, i.e., down-regulation of the L1Rn B6 repetitive DNA element in females, and up-regulation of the LINE retrotransposable element 3 in males. Among those showing male-biased expression, there was only one with altered expression due to both EB and FA. MT1a transcripts showed up-regulation by EB in females and also by FA in males.

Fig. 5 shows mRNA expression data for two genes by real-time RT-PCR regarding sex differences in the neonatal MPOAs observed with microarrays. Both thymosin $\beta 4$ and Gαi2 mRNAs exhibited strong male-biased expression at PND 2, with 8.9- and 7.1-fold higher levels than in females. Real-time RT-PCR results confirmed this sex difference.

Immunoreactivity of Protein Signals

Fig. 6 shows representative figures for immunohistochemical demonstration of protein signals in the MPOA with the anatomical location indicated in

Table 4 List of Genes Showing Altered Expression in the MPOA of Both Sexes by EB-Treatment (≥2-fold, $p < 0.05$)

			Altered by EB (× fold *vs.* control)	
Accession No.	Gene	Sex Difference (× fold)	M	F
M13100	LINE retrotransposable element 3	M<F (2.9)	2.1	0.5
X07686	L1Rn B6 repetitive DNA element	M<F (3.8)	2.0	0.4
AA964849	ADP-ribosyltransferase (adprt) 1	M<F (3.3)	2.2	0.3
AF036335	NonO/p54nrb homolog	M<F (5.5)	3.2	<0.1

MPOA, medial preoptic area; EB, estradiol benzoate; FA, flutamide; M, males; F, females; EST, expressed sequence tag.

Table 5 List of Genes Showing Altered Expression in the MPOA Common to EB and FA (≥2-fold, $p < 0.05$)

Accession No.	Gene	Sex Difference (× fold)	Altered by EB (× fold *vs.* control)		Altered by FA (× fold *vs.* control)	
			M	F	M	F
M13100	LINE retrotransposable element 3	M<F (2.9)	2.1	0.5	2.2	–
U87960	Protein tyrosine phosphatase, receptor type, F (PTPRF); leukocyte common antigen receptor (LAR)	M<F (11.8)	–	0.1	–	0.4
AJ006971	DAP-like kinase (dlk)	M<F (6.4)	–	0.3	–	0.3
U08257 (X59996)	Glutamate receptor, ionotropic, kainite 4 (Grik4); Kainate receptor subunit (KA1)	M<F (5.8)	–	0.3	–	0.5
		(M<F (5.4))	(–)	(0.2)	(–)	(0.5)
AA892562	Dyskeratosis congenita 1, dyskerin (dkc1)	M<F (4.0)	–	0.4	–	0.4
X07686	L1Rn B6 repetitive DNA element	M<F (3.8)	2.0	0.4	–	0.2
X53455	Microtubule-associated protein 2 (MAP2)	M<F (3.5)	–	0.1	–	0.3
AA859593	EST, similar to mouse estrogen-responsive finger protein (efp)	M<F (3.4)	–	0.3	–	0.5
X17184	Glutamate receptor, ionotropic, AMPA subtype, GluR1	M<F (3.1)	–	0.3	–	0.5
AJ006295	Myeloid/lymphoid or mixed-lineage leukemia (trithorax (Drosophila) homolog); translocated to, 3 (mllt3); AF-9	–	–	0.4	–	0.5
AI231257	Cyclin D1	–	–	0.4	–	0.5
AA799791	Serine/threonine kinase 25 (STE20 homolog, yeast) (stk25)	–	–	0.4	–	0.4
U16845	Neurotrimin	–	–	0.5	–	0.5
AI639097	EST	–	–	2.2	–	0.5
AI176456	Metallothionein (MT1a)	M>F (2.8)	–	2.9	2.3	–

MPOA, medial preoptic area; EB, estradiol benzoate; FA, flutamide; M, males; F, females; EST, expressed sequence tag.

Figure 1. In the hypothalamus at PND 2, nuclear immunoreactivity of PARP, the protein product of the *adprt* gene (Skaper, 2003), was observed in the ventricular ependymal and subependymal cells around the third ventricle. On quantitative measurement of nuclear immunoreactivity at the SDN region, cases with higher grades of distribution were more frequent in female controls when compared with the males [Figs. 6(A,B) and 7]. EB-treatment increased and decreased the positive cell distribution in males and females, respectively [Figs. 6(C) and 7]. GluR1 immunoreactivity was observed in the cytoplasm and dendritic processes of neuronal cells, its staining intensity being mostly weak in the MPOAs, even in the positive cases, when compared with the other brain areas, such as the hippocampus, cerebral cortex, and striatum [Fig. 6(D)]. In the MPOAs of male controls, two out of four cases showed only minimal intensity of GluR1-immunoreactivity, and the other two showed negative results [Fig. 6(D), Table 6]. Although the intensity was minimal to slight, all control females showed positive immunoreactivity in their MPOAs [Fig. 6(E)]. EB-treatment did not alter the intensity in either sex [female: Fig. 6(F)]. With regard to GluR5, very faint immunoreactivity was observed in the dendritic processes in the striatum and bed nucleus, but staining was lacking in the MPOAs of both sexes, even with the EB treatment

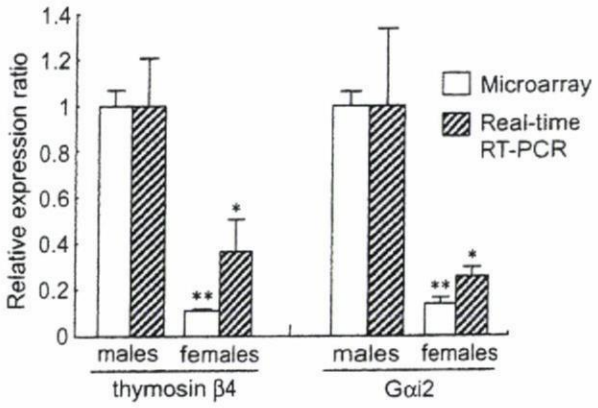

Figure 5 Confirmation of microarray data by real-time RT-PCR in the neonatal MPOA. Sex differences in the mRNA expression of thymosin $\beta 4$ and $G\alpha i2$ were analyzed. Significantly different from the male value in each detection system ($*p < 0.05$, $**p < 0.01$).

(Table 6). GluR6/7-immunoreactivity was observed in the cytoplasm of both neuronal and glial cells of the whole brain area, but there was no obvious change in terms of the distribution and intensity in the MPOAs, irrespective of the sex or EB treatment (Table 6). MAP2 immunoreactivity was observed in the whole dendritic processes with a fibrillary expression pattern, but there was no obvious change in terms of the distribution and intensity in the MPOAs, irrespective of the sex or EB treatment (Table 6). Strong cytoplasmic immunoreactivity of MT-1/2 was observed in the astrocytes located in the deep cortex and white matter of the cerebrum, hippocampal white matter, and striatum [Fig. 6(G)]. In other brain areas, MT-1/2-immunoreactivity was rather weak and sparse, and both nuclear and cytoplasmic. In the MPOAs, nuclear immunoreactivity predominated over cytoplasmic staining. On quantitative measurement of the nuclear immunoreactivity, the positive cell ratio was higher in males than in females, with increase in the latter on EB treatment [Figs. 6(G–I) and 7].

DISCUSSION

In the present validation study to establish a region-specific microarray analysis method using PET samples in combination with methacarn fixation, we found that gene expression profiles were very similar between 2×-amplified aRNAs from UFT and methacarn-fixed PET, and the deviation in expression data with the second-round amplification from the 1×-amplified aRNAs of UFT was mostly due to the preferential amplification of the 3′-terminal portion, irrespective of the tissue status. These results strongly indicate that methacarn fixation and subsequent paraffin embedding do not affect the expression fidelity in microarray analyses. Although it is still necessary to improve expression fidelity with second-round amplification, the results suggest an advantage of methacarn in combination with paraffin embedding for global gene expression analysis of microdissected cellular regions. It should be stressed that paraffin embedding is essential for preparation of serial sections necessary for microdissection of anatomically defined tissue areas.

Although the sex difference in the incidence of apoptosis in the SDN region that is believed to be re-

Figure 6 Immunoexpression patterns for PARP (panels A-C), GluR1 (panels D-F), and MT-1/2 (panels G-I), in the neonatal rat MPOA at PND 2. A. Note scattered PARP-immunoreactive nuclei (arrowheads) in paraventricular cells of a control male. The inset shows a high-power view of the nuclear weak immunoreactivity in the same area. B. Distribution of PARP-weakly immunoreactive cell nuclei in a control female. Note accumulation of positive cells in the SDN region (arrow). C. Lack of PARP-immunoreactive cells in most paraventricular and SDN regions in an EB-treated female. D. Very weak, mostly negative GluR1-immunoreactivity in the cytoplasmic processes of neurons in a control male. The inset shows strong immunoreactivity in the cytoplasm and dendritic processes of neuronal cells of the cerebral cortex of the same brain section. E. Slight intensity of GluR1-immunoreactivity in cytoplasmic processes of neurons in a control female. The inset shows a high-power view of the immunoreactivity in cytoplasmic processes of the same area. F. Minimal degree of GluR1-immunoreactivity in an EB-treated female. G. Diffuse immunoexpression of MT-1/2 in a control male. The expression pattern is mostly nuclear, and both astrocytic (arrowheads) and neuronal (arrows) populations as well as ependymal cells (*) show apparent immunoreactivity. The inset shows strong expression in cytoplasmic processes of astrocytes in the deep cerebral cortex of the same brain section. H. Scattered weak nuclear immunoreactivity of MT-1/2 in a control female. I. Diffuse nuclear and scattered cytoplasmic distribution of immunoreactive cells in an EB-treated female. The inset shows a high power view of both nuclear and cytoplasmic immunoreactivity in the same area. Bar = 50 μm, including insets.

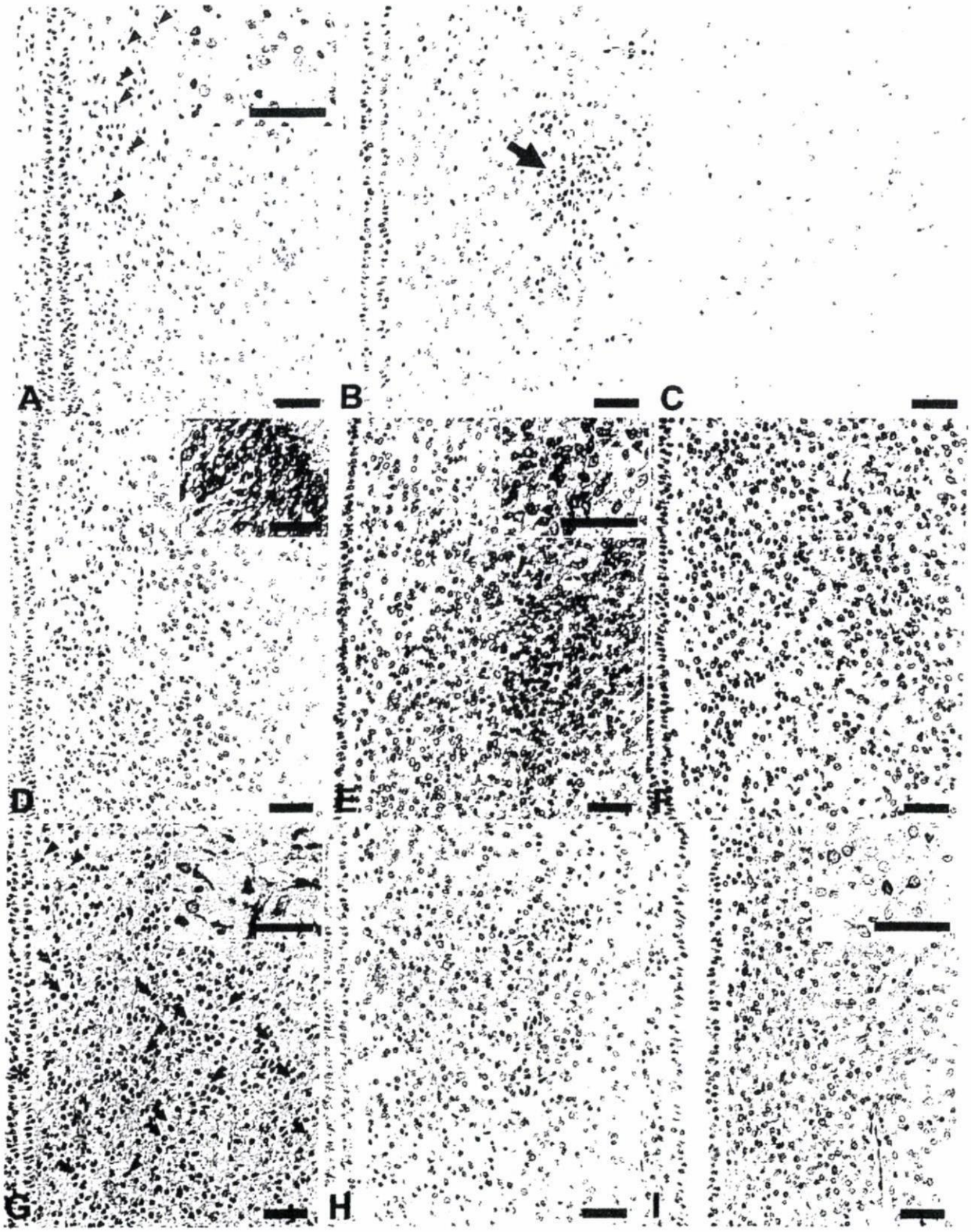

Figure 6

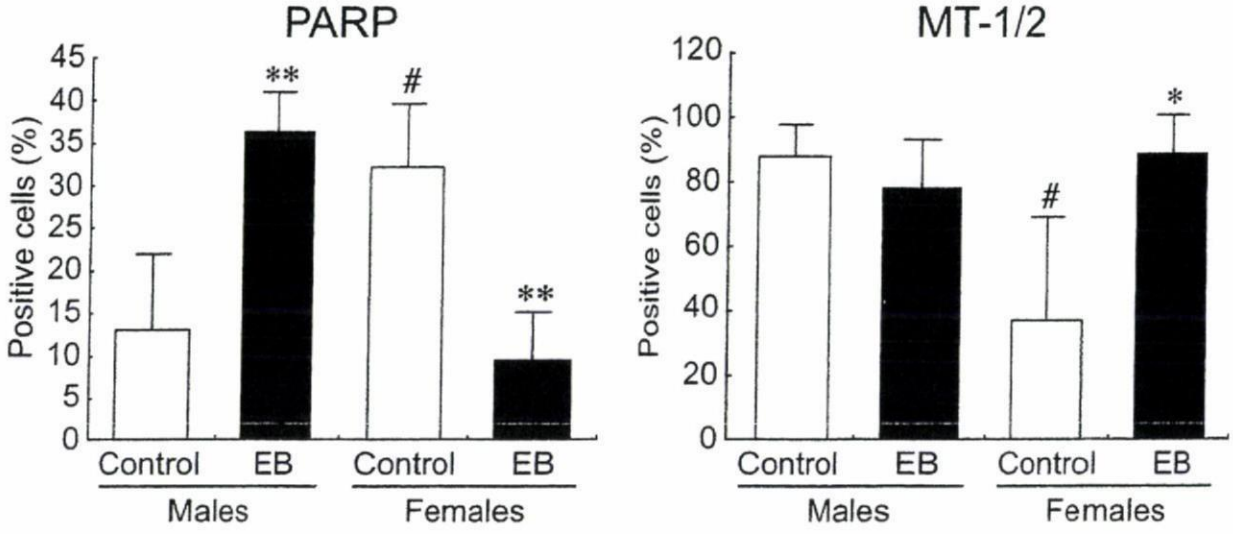

Figure 7 Nuclear immunoreactive cell percentages for PARP and MT-1/2 in neonatal rat MPOAs at PND 2. Significantly different from the corresponding controls ($^{*}p < 0.05$, $^{**}p < 0.01$). Significantly different from the male controls ($^{\#}p < 0.05$).

sponsible for subsequent sexually dimorphic development of this nucleus first occurs between PNDs seven and 10 (Davis et al., 1996), the number of genes exhibiting male-biased constitutive expression was much higher than in females at time points as early as PND 2 in the present study. This sex difference is presumably the reflection of growth and/or antiapoptotic effects for male-type large SDN under the influence of estradiol generated by aromatase from testosterone perinatally secreted from the developing testis (Matsumoto et al., 2000). Regarding responses to chemicals, the number of genes showing altered expression by EB or FA was far greater in females than in males, suggesting an effect on normal female sexual differentiation. Moreover, approximately 60% of genes showing male or female-biased expression demonstrated altered levels with EB in females, pointing to an involvement of genes necessary for normal processes of male- or female-type brain sexual differentiation in its disruptive effects. It is well known that the perinatal/neonatal treatment of animals with estrogenic compounds can affect sexual development of both sexes, resulting in reproductive dysfunction (Nagao et al., 1999; Odum et al., 2002; Tsukahara et al., 2003; Shibutani et al., 2005). With regard to the effects of antiandrogens, disruption of sexual development has generally been apparent in males, but the situation is largely unclear for females (Gray and Kelce, 1996; Wolf et al., 2004). With FA, however, prenatal exposure affects the volume of the anteroventral periventricular nucleus (AVPVN) in female rats (Lund et al., 2000) and the female sexual behavior in guinea pigs (Thornton et al., 1991). In addition, FA exerts antiprogestin activity (Chandrasekhar and Armstrong, 1989; Dukes et al., 2000).

Table 6 Immunoreactivity of Protein Signals in the MPOA of Neonatal Rats Treated with EB[a]

	Males		Females	
Antigen	Control	EB	Control	EB
Number of animals	4	4	4	4
GluR1 (±/+)[b]	2[c](2/0)[d]	3(3/0)	4(3/1)	3(3/0)
GluR5 (present)	0	0	0	0
GluR6/7 (±/+/++)[b]	4(2/2/0)	4(0/4/0)	4(0/3/1)	4(2/2/0)
MAP2 (±/+/++)[b]	4(0/3/1)	4(0/3/1)	4(2/2/0)	4(2/2/0)

Protein signals with immunoexpression patterns for which morphometric analysis could not be applied were analyzed by visual estimation of the grade of intensity of immunoreactivity in the MPOA. MPOA, medial preoptic area; EB, estradiol benzoate; GluR1, glutamate receptor 1; GluR5, glutamate receptor 5; GluR6/7; glutamate receptor 6/7; MAP2, microtubule-associated protein 2.

[a] Rat neonates treated with EB at 10 μg/pup or vehicle on PND1 and sacrificed 24 h later were examined.

[b] Grades of intensity of immunoreactivity: ±, minimal; +, slight; ++, moderate; and +++, prominent.

[c] Total number of animals showing positive immunoreactivity.

[d] Number of animals with each grade.

Our search for genes showing altered expression by EB or FA revealed a total of four female-predominant genes with change by EB in both sexes, all up-regulated in males and down-regulated in females. Two of them are long interspersed repetitive DNAs, L1, or LINE, a class of mobile genetic elements named retrotransposons which can be amplified by retroposition, i.e. by a mechanism similar to that observed with retroviruses (Servomaa and Rytoamaa,

1990). This group of retrotransposons includes regulatory signals and encodes two proteins, a RNA-binding protein and an integrase-replicase (Han and Boeke, 2005). The human genome contains about 500,000 LINES, accounting for roughly 17% of the total (Haoudi et al., 2004). Various environmental factors, such as steroid hormone-like agents and stressors can facilitate L1 transcription to alter cellular functions (Servomaa and Rytoamaa, 1990; Morales et al., 2002, 2003). Moreover, a regulatory role of L1 repeats at the promoter region has been reported with estrogen-related gene transcription (Hardy et al., 2001). During neuronal differentiation, retrotransposition events can alter the expression of neuronal genes, which, in turn, can influence neuronal cell fate (Muotri et al., 2005). Thus, the sex differences in the retrotransposon expression in the developing MPOA apparent here suggest roles in sex-dependent gene expression control, and alteration in their expression status due to EB may indicate roles as upstream regulators of genes necessary for brain sexual differentiation.

Two other genes showing up-regulation in males and down-regulation in females with EB, as well as female-biased expression, were *adprt1* and *NonO/p54nrb*. *Adprt1* encodes PARP-1, an abundant nuclear enzyme that is activated primarily by DNA damage; however, its excessive activation can lead to cell death (Skaper, 2003; Koh et al., 2005). Interestingly, sex differences exist regarding PARP-1 activation as well as nitric oxide toxicity in a mouse ischemic neurotoxicity model (McCullough et al., 2005). In the periventricular cell populations, poly(ADP-ribosyl)ation is basally activated by DNA strand breaks reflecting glutamate-nitric oxide neurotransmission (Pieper et al., 2000). In the present study, the measured level of PARP-immunoexpression at the SDN region was in line with the microarray data, suggesting an induction of subsequent programmed cell death in the female SDN-POA (Davis et al., 1996). Similarly, increased expression of PARP in males and its decrease in females with EB here may be linked to the decreased SDN volume in males in later life (Shibutani et al., 2005) and the decreased apoptosis in the female SDN after EB injection (Arai et al., 1996), respectively. NonO/p54nrb has been implicated in a variety of nuclear processes (Proteau et al., 2005). Indeed, this protein is known to act as a transcription factor necessary for adrenocortical steroidogenesis (Sewer et al., 2002), and as a transcriptional co-activator of the human androgen receptor (AR; Ishitani et al., 2003).

In the present study, a total of 15 genes exhibited altered expression due to FA in either sex, in addition to alteration by EB. Among them, 10 genes also exhibited sex differences in expression including the two genes for retrotransposons mentioned earlier. Interestingly, many of the 15 genes exhibited similar expression patterns with EB and FA, most being down-regulated in females, suggesting a common mechanism of action of the two chemicals. The following seven genes showed this particular expression pattern, in addition to the L1 repeat mentioned earlier: *PTPRF*/leukocyte common antigen-related (LAR) protein, *dlk*, two kinds of glutamate receptors, *dyskerin*, *MAP2*, and *efp*. In males, neonatal estrogen treatment affects the developing testis to suppress androgen secretion, presumably resulting in effects similar to antiandrogenicity on postnatal development (Atanassova et al., 1999). On the other hand, FA in the 20-day pubertal female assay using rats has been shown to exert ER-agonist activity on female sexual development, attributed to an imbalance between endogenous estrogenic and androgenic stimuli in the target organs (Kim et al., 2002).

Regarding glutamate receptors, mRNA expression of GluR1, the AMPA subtype found here with altered expression, is up-regulated in the AVPVN by estrogen in ovariectomized juvenile female rats (Gu et al., 1999). Hypothalamic GluR1 protein level was also increased in gonadectomized and estrogen-treated adult rats irrespective of the sex (Diano et al., 1997). Different from our female neonates, these results suggest that estrogen could up-regulate GluR1 levels in the juvenile/adult rat hypothalamus, probably through a different mechanism from that during sexual differentiation. In the female MPOA, we here could detect a slight, but nonsignificant increase in GluR1-immunoreactive cases when compared with those in males. Although we could not examine immunohistochemical localization of KA1 subunit here, other kainate receptor subtypes (GluR5, 6, and 7) have shown, in a study using adult rats, to be expressed in tanycytes, astrocytes, and neurons of the arcuate nucleus, with co-expression of AR or ER found in neurons in males and females, respectively (Diano et al., 1998). However, we could not detect any sex difference or EB-induced effect on the immunoreactivity of GluR5 or GluR6/7 in the neonatal MPOA.

PTPRF/LAR is a widely expressed tyrosine phosphatase that has been implicated in the regulation of a diverse range of signaling pathways, such as in the development and maintenance of excitatory synapses, and interestingly, disruption of its function results in reduction of surface AMPA receptors (Mooney and LeVea, 2003; Dunah et al., 2005). In the present study, AMPA subtype GluR1, as mentioned earlier, showed similar responses to EB and FA as well as a sex differ-

ence in mRNA expression, suggesting a coordinated action of PTPRF/LAR and AMPA receptors during brain sexual differentiation and its disruption.

MAP2 contributes to regulation of cytoskeletal organization and dynamics, and is expressed mainly in dendritic processes of neurons (Maccioni and Cambiazo, 1995). Posttranscriptional control of MAP2 expression has been reported in the female rat hippocampus in response to estrogen treatment or during the estrous cycle (Reyna-Neyra et al., 2002, 2004). Interestingly, estrogen can induce dendrite spines in the developing rat POA through activation of AMPA-kainate receptors by glutamate that may originate from astrocytes (Amateau and McCarthy, 2002). Inconsistent with the microarray data, MAP2-immunoreactivity in the neonatal MPOA here lacked any sex difference or change in expression on chemical treatment as in the case with above-mentioned GluR5 and GluR6/7.

Efp, a target gene product of ERα, is a RING-finger-dependent ubiquitin ligase that targets proteolysis of 14-3-3σ, a negative cell cycle regulator that causes G2 arrest (Urano et al., 2002), and is considered essential for estrogen-dependent tumor cell proliferation (Horie et al., 2003). This gene product is distributed mainly in estrogen-sensitive organs/tissues associated with ER co-expression (Orimo et al., 1995; Shimada et al., 2004). Dlk is a nuclear serine/threonine-specific kinase that has been implicated in the regulation of apoptosis by relocation to the cytoplasm, but its nuclear location has been suggestive of the roles for mitosis and cytokinesis (Preuss et al., 2003). Dyskerin, a nucleolar protein that modifies specific uridine residues of rRNA, also acting as a component of the telomerase complex, is a target molecule for skin and bone marrow failure syndrome called dyskeratosis congenita in human (Marrone et al., 2005). Dyskerin transcripts distribute ubiquitously in embryo-fetal tissues with notably high levels in epithelial and neural tissues (Heiss et al., 2000).

As a unique gene showing male-biased expression and increase with EB in females and decrease with FA in males, *MT1a* is of interest. MTs are considered to be important metal-binding proteins active in defense against heavy metal toxicity (Sogawa et al., 2001), and four major MT isoforms have so far been identified. In the present study, judging from the sequence information (accession no. AI176456) for the MT probes, either MT1 or 2 was suggested to be responsible for the particular expression pattern. Sex steroid-related expression changes in MT1 and/or 2 have been reported in the liver or brain of mice (Sogawa et al., 2001; Beltramini et al., 2004). In the brain, MT1 and 2 are expressed mainly in nonneuronal cells (Suzuki et al., 1994; Hidalgo et al., 2001), but certain levels are also found in neurons (Xie et al., 2004); as well as cytoplasmic expression, nuclear localization of MT has been reported in developing brain (Suzuki et al., 1994). Interestingly, kainic acid treatment can selectively induce MT1 in neurons and MT2 in glial cells in rats (Kim et al., 2003). Although the immunoreactivity of MT-1/2 was rather weak when compared with other brain areas and a nuclear expression was predominant in the neonatal MPOA here, male predominance may reflect a neuroprotective function, and expression changes due to EB and FA could indicate alteration in the regional hormonal environment in response to treatment.

In summary, we here established the basis for a global gene expression profiling method using paraffin-embedded, histologically defined small tissue areas with methacarn as a fixative. A male predominance in the number of genes showing constitutively higher expression suggestive of sex steroidal effects on the neonatal male MPOA was detected. Upon treatment with EB, many genes showing sex differences in expression demonstrated altered levels in females, in line with involvement of genes necessary for brain sexual differentiation in its disruption. Moreover, many genes commonly affected by EB and FA showed down-regulation in females with these drugs, suggesting common mechanisms shared between estrogenic and anti-androgenic chemicals in induction of endocrine center disruption in females, at least in early stages.

We thank Mrs. Keiko Kuroiwa for her technical assistance in conducting the immunohistochemical study. Dr. Lee was an Awardee of a Postdoctoral Fellowship from the Japan Society for the Promotion of Science during the performance of the study.

REFERENCES

Amateau SK, McCarthy MM. 2002. A novel mechanism of dendritic spine plasticity involving estradiol induction of prostaglandin-E_2. J Neurosci 22:8586–8596.

Arai Y, Sekine Y, Murakami S. 1996. Estrogen and apoptosis in the developing sexually dimorphic preoptic area in female rats. Neurosci Res 25:403–407.

Atanassova N, McKinnell C, Walker M, Turner KJ, Fisher JS, Morley M, Millar MR, et al. 1999. Permanent effects of neonatal estrogen exposure in rats on reproductive hormone levels, Sertoli cell number, and the efficiency of spermatogenesis in adulthood. Endocrinology 140:5364–5373.

Beltramini M, Zambenedetti P, Wittkowski W, Zatta P. 2004. Effects of steroid hormones on the Zn, Cu and MTI/II levels in the mouse brain. Brain Res 1013:134–141.

Chandrasekhar Y, Armstrong DT. 1989. Ability of progesterone to reverse anti-androgen (hydroxyflutamide)-induced interference with the preovulatory LH surge and ovulation in PMSG-primed immature rats. J Reprod Fertil 85:309–316.

Davis EC, Popper P, Gorski RA. 1996. The role of apoptosis in sexual differentiation of the rat sexually dimorphic nucleus of the preoptic area. Brain Res 734:10–18.

Diano S, Naftolin F, Horvath TL. 1997. Gonadal steroids target AMPA glutamate receptor-containing neurons in the rat hypothalamus, septum and amygdala: A morphological and biochemical study. Endocrinology 138:778–789.

Diano S, Naftolin F, Horvath TL. 1998. Kainate glutamate receptors (GluR5-7) in the rat arcuate nucleus: Relationship to tanycytes, astrocytes, neurons and gonadal steroid receptors. J Neuroendocrinol 10:239–247.

Dukes M, Furr BJ, Hughes LR, Tucker H, Woodburn JR. 2000. Nonsteroidal progestins and antiprogestins related to flutamide. Steroids 65:725–731.

Dunah AW, Hueske E, Wyszynski M, Hoogenraad CC, Jaworski J, Pak DT, Simonetta A, et al. 2005. LAR receptor protein tyrosine phosphatases in the development and maintenance of excitatory synapses. Nat Neurosci 8:458–467.

Gray LE Jr, Kelce WR. 1996. Latent effects of pesticides and toxic substances on sexual differentiation of rodents. Toxicol Ind Health 12:515–531.

Gu G, Varoqueaux F, Simerly RB. 1999. Hormonal regulation of glutamate receptor gene expression in the anteroventral periventricular nucleus of the hypothalamus. J Neurosci 19:3213–3222.

Han JS, Boeke JD. 2005. LINE-1 retrotransposons: Modulators of quantity and quality of mammalian gene expression? Bioessays 27:775–784.

Haoudi A, Semmes OJ, Mason JM, Cannon RE. 2004. Retrotransposition-competent human LINE-1 induces apoptosis in cancer cells with intact p53. J Biomed Biotechnol 2004:185–194.

Hardy DO, Niu EM, Catterall JF. 2001. Kap promoter analysis *in vivo*: A regulatory role for a truncated L1 repeat. Mol Cell Endocrinol 181:57–67.

Heiss NS, Bächner D, Salowsky R, Kolb A, Kioschis P, Poustka A. 2000. Gene structure and expression of the mouse dyskeratosis congenita gene, *dkc1*. Genomics 67: 153–163.

Hidalgo J, Aschner M, Zatta P, Vasak M. 2001. Roles of the metallothionein family of proteins in the central nervous system. Brain Res Bull 55:133–145.

Horie K, Urano T, Ikeda K, Inoue S. 2003. Estrogen-responsive RING finger protein controls breast cancer growth. J Steroid Biochem Mol Biol 85:101–104.

Ishitani K, Yoshida T, Kitagawa H, Ohta H, Nozawa S, Kato S. 2003. p54nrb acts as a transcriptional coactivator for activation function 1 of the human androgen receptor. Biochem Biophys Res Commun 306:660–665.

Kim D, Kim EH, Kim C, Sun W, Kim HJ, Uhm CS, Park SH, et al. 2003. Differential regulation of metallothionein-I, II, and III mRNA expression in the rat brain following kainic acid treatment. Neuroreport 14:679–682.

Kim HS, Shin JH, Moon HJ, Kim TS, Kang IH, Seok JH, Kim IY, et al. 2002. Evaluation of the 20-day pubertal female assay in Sprague-Dawley rats treated with DES, tamoxifen, testosterone, and flutamide. Toxicol Sci 67: 52–62.

Kocarek TA, Kraniak JM, Reddy AB. 1998. Regulation of rat hepatic cytochrome P450 expression by sterol biosynthesis inhibition: Inhibitors of squalene synthase are potent inducers of CYP2B expression in primary cultured rat hepatocytes and rat liver. Mol Pharmacol 54:474–484.

Koh DW, Dawson TM, Dawson VL. 2005. Poly(ADP-ribosyl)ation regulation of life and death in the nervous system. Cell Mol Life Sci 62:760–768.

Lund TD, Salyer DL, Fleming DE, Lephart ED. 2000. Pre or postnatal testosterone and flutamide effects on sexually dimorphic nuclei of the rat hypothalamus. Brain Res Dev Brain Res 120:261–266.

Maccioni RB, Cambiazo V. 1995. Role of microtubule-associated proteins in the control of microtubule assembly. Physiol Rev 75:835–864.

Marrone A, Walne A, Dokal I. 2005. Dyskeratosis congenita: Telomerase, telomeres and anticipation. Curr Opin Genet Dev 15:249–257.

Masutomi N, Shibutani M, Takagi H, Uneyama C, Takahashi N, Hirose M. 2003. Impact of dietary exposure to methoxychlor, genistein, or diisononyl phthalate during the perinatal period on the development of the rat endocrine/reproductive systems in later life. Toxicology 192: 149–170.

Matsumoto A, Sekine Y, Murakami S, Arai Y. 2000. Sexual differentiation of neuronal circuitry in the hypothalamus. In: Matsumoto A, editor. Sexual Differentiation of the Brain. Boca Raton: CRC Press, pp 203–227.

McCullough LD, Zeng Z, Blizzard KK, Debchoudhury I, Hurn PD. 2005. Ischemic nitric oxide and poly (ADP-ribose) polymerase-1 in cerebral ischemia: Male toxicity, female protection. J Cereb Blood Flow Metab 25:502–512.

McEwen BS, Alves SE. 1999. Estrogen actions in the central nervous system. Endocr Rev 20:279–307.

Meisel RL, Sachs BD. 1994. The physiology of male sexual behavior. In: Knobil E, Neills JD, editors. The Physiology of Reproduction, 2nd ed. New York: Raven Press, pp 3–106.

Meredith JM, Bennett C, Scallet AC. 2001. A practical three-dimensional reconstruction method to measure the volume of the sexually-dimorphic central nucleus of the medial preoptic area (MPOC) of the rat hypothalamus. J Neurosci Methods 104:113–121.

Mooney RA, LeVea CM. 2003. The leukocyte common antigen-related protein LAR: Candidate PTP for inhibitory targeting. Curr Top Med Chem 3:809–819.

Morales JF, Snow ET, Murnane JP. 2002. Environmental factors affecting transcription of the human L1 retrotransposon. I. Steroid hormone-like agents. Mutagenesis 17:193–200.

Morales JF, Snow ET, Murnane JP. 2003. Environmental factors affecting transcription of the human L1 retrotransposon. II. Stressors. Mutagenesis 18:151–158.

Muotri AR, Chu VT, Marchetto MC, Deng W, Moran JV, Gage FH. 2005. Somatic mosaicism in neuronal precursor cells mediated by L1 retrotransposition. Nature 435:903–910.

Nagao T, Saito Y, Usumi K, Kuwagata M, Imai K. 1999. Reproductive function in rats exposed neonatally to bisphenol A and estradiol benzoate. Reprod Toxicol 13:303–311.

Numan M. 1994. Maternal behavior. In: Knobil E, Neills JD, editors. The Physiology of Reproduction, 2nd ed. New York: Raven Press, pp 221–302.

Odum J, Lefevre PA, Tinwell H, Van Miller JP, Joiner RL, Chapin RE, Wallis NY, et al. 2002. Comparison of the developmental and reproductive toxicity of diethylstilbestrol administered to rats *in utero*, lactationally, preweaning, or postweaning. Toxicol Sci 68:147–163.

Orikasa C, Kondo Y, Hayashi S, McEwen BS, Sakuma Y. 2002. Sexually dimorphic expression of estrogen receptor β in the anteroventral periventricular nucleus of the rat preoptic area: Implication in luteinizing hormone surge. Proc Natl Acad Sci USA 99:3306–3311.

Orimo A, Inoue S, Ikeda K, Noji S, Muramatsu M. 1995. Molecular cloning, structure, and expression of mouse estrogen-responsive finger protein Efp. Co-localization with estrogen receptor mRNA in target organs. J Biol Chem 270:24406–24413.

Pieper AA, Blackshaw S, Clements EE, Brat DJ, Krug DK, White AJ, Pinto-Garcia P, et al. 2000. Poly(ADP-ribosyl) ation basally activated by DNA strand breaks reflects glutamate-nitric oxide neurotransmission. Proc Natl Acad Sci USA 97:1845–1850.

Preuss U, Bierbaum H, Buchenau P, Scheidtmann KH. 2003. DAP-like kinase, a member of the death-associated protein kinase family, associates with centrosomes, centromers, and the contractile ring during mitosis. Eur J Cell Biol 82:447–459.

Proteau A, Blier S, Albert AL, Lavoie SB, Traish AM, Vincent M. 2005. The multifunctional nuclear protein p54nrb is multiphosphorylated in mitosis and interacts with the mitotic regulator Pin1. J Mol Biol 346:1163–1172.

Reyna-Neyra A, Arias C, Ferrera P, Morimoto S, Camacho-Arroyo I. 2004. Changes in the content and distribution of microtubule associated protein 2 in the hippocampus of the rat during the estrous cycle. J Neurobiol 60:473–480.

Reyna-Neyra A, Camacho-Arroyo I, Ferrera P, Arias C. 2002. Estradiol and progesterone modify microtubule associated protein 2 content in the rat hippocampus. Brain Res Bull 58:607–612.

Rhees RW, Shryne JE, Gorski RA. 1990a. Onset of the hormone-sensitive perinatal period for sexual differentiation of the sexually dimorphic nucleus of the preoptic area in female rats. J Neurobiol 21:781–786.

Rhees RW, Shryne JE, Gorski RA. 1990b. Termination of the hormone-sensitive period for differentiation of the sexually dimorphic nucleus of the preoptic area in male and female rats. Dev Brain Res 52:17–23.

Rivas A, Fisher JS, McKinnell C, Atanassova N, Sharpe RM. 2002. Induction of reproductive tract developmental abnormalities in the male rat by lowering androgen production or action in combination with a low dose of diethylstilbestrol: Evidence for importance of the androgen-estrogen balance. Endocrinology 143:4797–4808.

Servomaa K, Rytomaa T. 1990. UV light and ionizing radiations cause programmed death of rat chloroleukaemia cells by inducing retropositions of a mobile DNA element (L1Rn). Int J Radiat Biol 57:331–343.

Sewer MB, Nguyen VQ, Huang CJ, Tucker PW, Kagawa N, Waterman MR. 2002. Transcriptional activation of human CYP17 in H295R adrenocortical cells depends on complex formation among p54nrb/NonO, protein-associated splicing factor, and SF-1, a complex that also participates in repression of transcription. Endocrinology 143:1280–1290.

Shibutani M, Masutomi N, Uneyama C, Abe N, Takagi H, Lee KY, Hirose M. 2005. Down-regulation of GAT-1 mRNA expression in the microdissected hypothalamic medial preoptic area of rat offspring exposed maternally to ethinylestradiol. Toxicology 208:35–48.

Shibutani M, Uneyama C. 2002. Methacarn: A fixation tool for multipurpose genetic analysis from paraffin-embedded tissues. In: Conn M, editor. Methods in Enzymology, Vol. 356. New York: Academic Press, pp 114–125.

Shibutani M, Uneyama C, Miyazaki K, Toyoda K, Hirose M. 2000. Methacarn fixation: A novel tool for analysis of gene expressions in paraffin-embedded tissue specimens. Lab Invest 80:199–208.

Shimada N, Suzuki T, Inoue S, Kato K, Imatani A, Sekine H, Ohara S, et al. 2004. Systemic distribution of estrogen-responsive finger protein (Efp) in human tissues. Mol Cell Endocrinol 218:147–153.

Skaper SD. 2003. Poly(ADP-ribose) polymerase-1 in acute neuronal death and inflammation: A strategy for neuroprotection. Ann NY Acad Sci 993:217–228; discussion 287–288.

Sogawa N, Sogawa CA, Oda N, Fujioka T, Onodera K, Furuta H. 2001. The effects of ovariectomy and female sex hormones on hepatic metallothionein-I gene expression after injection of cadmium chloride in mice. Pharmacol Res 44:53–57.

Suzuki K, Nakajima K, Otaki N, Kimura M. 1994. Metallothionein in developing human brain. Biol Signals 3:188–192.

Takagi H, Shibutani M, Kato N, Fujita H, Lee KY, Takigami S, Mitsumori K, et al. 2004. Microdissected region-specific gene expression analysis with methacarn-fixed, paraffin-embedded tissues by real-time RT-PCR. J Histochem Cytochem 52:903–913.

Tena-Sempere M, Gonzalez LC, Pinilla L, Huhtaniemi I, Aguilar E. 2001. Neonatal imprinting and regulation of estrogen receptor α and β mRNA expression by estrogen in the pituitary and hypothalamus of the male rat. Neuroendocrinology 73:12–25.

Thornton JE, Irving S, Goy RW. 1991. Effects of prenatal antiandrogen treatment on masculinization and defeminization of Guinea pigs. Physiol Behav 50: 471–475.

ukahara S, Ezawa N, Yamanouchi K. 2003. Neonatal estrogen decreases neural density of the septum-midbrain central gray connection underlying the lordosis-inhibiting system in female rats. Neuroendocrinology 78:226–233.

ıeyama C, Shibutani M, Masutomi N, Takagi H, Hirose M. 2002. Methacarn fixation for genomic DNA analysis in microdissected, paraffin-embedded tissue specimens. J Histochem Cytochem 50:1237–1245.

ano T, Saito T, Tsukui T, Fujita M, Hosoi T, Muramatsu M, Ouchi Y, et al. 2002. Efp targets 14-3-3σ for proteolysis and promotes breast tumour growth. Nature 417: 871–875.

Wolf CJ, LeBlanc GA, Gray LE Jr. 2004. Interactive effects of vinclozolin and testosterone propionate on pregnancy and sexual differentiation of the male and female SD rat. Toxicol Sci 78:135–143.

Xie T, Tong L, McCann UD, Yuan J, Becker KG, Mechan AO, Cheadle C, et al. 2004. Identification and characterization of metallothionein-1 and -2 gene expression in the context of (±)3, 4-methylenedioxymethamphetamine-induced toxicity to brain dopaminergic neurons. J Neurosci 24:7043–7050.

BIOCHEMICAL PHARMACOLOGY XXX (2008) XXX–XXX

available at www.sciencedirect.com

ScienceDirect

journal homepage: www.elsevier.com/locate/biochempharm

Review

AhR protein trafficking and function in the skin

Togo Ikuta [a,*], *Takeshi Namiki* [b], *Yoshiaki Fujii-Kuriyama* [c,d], *Kaname Kawajiri* [a,d]

[a] *Research Institute for Clinical Oncology, Saitama Cancer Center, 818 Komuro, Ina-machi, Kitaadachi-gun, Saitama 362-0806, Japan*
[b] *Department of Dermatology, School of Medicine, Tokyo Medical and Dental University, 1-5-45 Yushima, Bunkyo-ku, Tokyo 113-8510, Japan*
[c] *Center for Tsukuba Advanced Research Alliance, University of Tsukuba, 1-1-1 Tennodai, Tsukuba 305-8577, Japan*
[d] *Solution Oriented Research for Science and Technology (SORST), Japan Science and Technology Agency, 4-1-8 Honmachi, Kawaguchi, Saitama 331-0012, Japan*

ARTICLE INFO

Article history:
Received 8 July 2008
Accepted 3 October 2008

Keywords:
Subcellular localization
Cell–cell contact
Epithelial–mesenchymal transitions
Wound healing
Carcinogenesis

ABSTRACT

Because aryl hydrocarbon receptor (AhR) is a ligand-activated transcription factor, its nuclear translocation in response to ligands may be directly linked to transcriptional activation of target genes. We have investigated the biological significance of AhR from the perspective of its subcellular localization and revealed that AhR possesses a functional nuclear localization signal (NLS) as well as a nuclear export signal (NES) which controls the distribution of AhR between the cytoplasm and nucleus. The intracellular localization of AhR is regulated by phosphorylation of amino acid residues in the vicinity of the NLS and NES. In cell culture systems, cell density affects not only its intracellular distribution of AhR, but also its transactivation activity of the target genes such as transcriptional repressor Slug, which is important for the induction of epithelial–mesenchymal transitions. These effects of AhR observed in cultured cells are proposed to be reflected on the *in vivo* response such as morphogenesis and tumor formation.

This review summarizes recent work on the control mechanism of AhR localization and progress in understanding the physiological role of AhR in the skin. We propose that AhR is involved in normal skin formation during fetal development as well as in pathological states such as epidermal wound healing and skin carcinogenesis.

Contents

* *Corresponding author*. Tel.: +81 48 722 1111; fax: +81 48 722 1739.
E-mail address: togo@cancer-c.pref.saitama.jp (T. Ikuta).

0006-2952/$ – see front matter © 2008 Elsevier Inc. All rights reserved.
doi:10.1016/j.bcp.2008.10.003

Please cite this article in press as: Ikuta T, et al. AhR protein trafficking and function in the skin. Biochem Pharmacol (2008), doi:10.1016/j.bcp.2008.10.003

1. Introduction

The aryl hydrocarbon receptor (AhR) is a ligand-activated transcription factor with basic-helix-loop-helix (bHLH)/PER-ARNT-SIM homology region (PAS) family and is constitutively expressed in various mammalian tissues including lung, liver, thymus, and kidney [1]. AhR is involved in skin carcinogenesis by benzo[a]pyrene [2], teratogenesis in cleft palate [3], and hepatotoxicity [4]. Moreover, recent studies suggest that AhR plays a role in physiological function including immunity [5,6] and reproduction [7,8].

When environmental pollutants such as 2,3,7,8-tetrachlorodibenzo-*p*-dioxin (TCDD) and 3-methylcholanthrene bind to AhR, the ligand-activated AhR translocates to the nucleus where it binds to its heterodimerization partner AhR nuclear translocator (ARNT) [9]. The heterodimer AhR/ARNT binds to xenobiotic responsive elements, which are enhancer DNA elements located in the 5′-flanking region of the target genes [10]. While AhR activation by exogenous ligands is well investigated, very little is known about the physiological activation of AhR. Many studies using suspension cultures of various cell lines exist to show that AhR-mediated gene expression can be activated in the absence of exogenous ligands [11–13]. When adherent cells are suspended, intracellular signaling may be triggered by the loss of cell–cell contact or cell adhesion. This activation mechanism provides a model to investigate how AhR is activated under the normal physiological conditions.

Exposure to polycyclic aromatic hydrocarbons or topical application of these chemicals elicits inflammatory skin disease [14] as well as tumor formation [15]. This observation suggests that skin may provide clues to elucidate the biological function of AhR. The skin is a dynamic, regenerating organ. When skin is injured, various types of cells including leukocytes, fibroblasts and keratinocytes engage in tissue remodeling [16]. We attempted to study the role of AhR in the wound healing process. In benzo[a]pyrene skin carcinogenesis, it has been reported that AhR −/− mice do not develop tumors [2]. Since stem cells are considered to be the targets for carcinogens, it is very interesting to consider how AhR functions in stem cells. We are also going to discuss the possible roles of AhR on skin carcinogenesis.

2. AhR is a nucleo-cytoplasmic shuttling protein

AhR is a ligand-activated transcription factor and regulates biological responses to a variety of environmental contaminants. When exogenous ligands such as TCDD, benzo[a]pyrene, and 3-methylcholanthrene bind to AhR in cytoplasm, AhR translocates from the cytosol to the nucleus. It is important to investigate the localization of a transcription factor since change in its location is considered to impact gene regulation. Nuclear localization of a lot of nuclear proteins is determined by the nuclear localization signal (NLS) which is used for transport of these proteins to the nucleus through the nuclear pore complex [17,18]. This signal consists of a few short sequences of positively charged amino acid residues, whereas the nuclear export signal (NES) is a short leucine-rich sequence. We identified both the NLS 13–39 amino acid residues and NES 55–75 amino acid residues in the N-terminal region of AhR [19]. AhR shuttles between the cytoplasm and nucleus using these short peptide signals [20,21]. Subcellular localization of the shuttling protein is determined by the balance between nuclear import and nuclear export. It is reported that the localization is regulated by phosphorylation and dephosphorylation especially of amino acids close to the NLS or NES [22,23]. We found that the ligand-dependent nuclear import of AhR is inhibited by the substitution of aspartic acid for serine-12 or Ser-36, which mimics the negative charge conferred by phosphorylation [24]. It is likely that nuclear import of AhR is regulated by phosphorylation of NLS.

Distribution of AhR in a cell is controlled by its binding protein (Fig. 1). The unliganded AhR exists in cytosolic component as a complex [25], composed of AhR, a dimer of hsp90, p23, and the immunophilin homolog XAP2 [26,27]. XAP2 overexpression in cells is shown to enhance cytoplasmic AhR levels, suggesting that XAP2 is able to stabilize and enhance cellular levels of AhR [28,29]. Petrulis et al. [30] studied the mechanism of cytoplasmic retention of the AhR in the presence of XAP2. They showed that XAP2 hinders the binding of importin β to the AhR complex and proposed that XAP2 alters the conformation of the NLS. In addition, Berg and Pongratz [31] identified the other mechanism of XAP2-induced cytoplasmic localization of AhR. In particular, they showed that XAP2 anchors unliganded AhR to actin filaments since an actin inhibitor, cytochalasin B, blocked this effect.

Several reports demonstrate that the AhR is rapidly degraded via the proteasome pathway following exposure to ligands [32,33]. Davarinos and Pollenz [34] evaluated the function of the NES in the context of AhR degradation. They showed TCDD-induced degradation of the AhR was completely inhibited in the HepG2 cells pretreated with leptomycin B, an inhibitor of nuclear transport mediated by CRM1 (chromosomal maintenance factor 1) [35]. Furthermore, expressed AhR ΔNES protein was degraded to a lesser extent than wild-type AhR [34]. These data suggest that ligand-dependent degradation of AhR is mediated by nuclear export of AhR.

3. Cell density affects AhR localization and activity

We have shown that AhR is a nuclear-cytoplasmic shuttling protein. How are these transport mechanisms regulated under the physiological conditions ? We investigated stimuli that affect AhR localization using the human keratinocyte cell line HaCaT in the absence of exogenous ligand [36]. Because growth and differentiation of the cultured keratinocytes is regulated in part by cell density [37,38], effects of cell density on AhR localization were examined. When cells were sparsely inoculated, AhR was predominantly localized in the nucleus. When the cells were subconfluent, AhR was distributed equally both in cytoplasm and nucleus. However, when cells were fully confluent, immunostained AhR was localized predominantly in the cytoplasm. It is suggested that nuclear translocation of AhR is negatively regulated by phosphorylation of serine residues located in its NLS [24]. It is possible that

Please cite this article in press as: Ikuta T, et al. AhR protein trafficking and function in the skin. Biochem Pharmacol (2008), doi:10.1016/j.bcp.2008.10.003

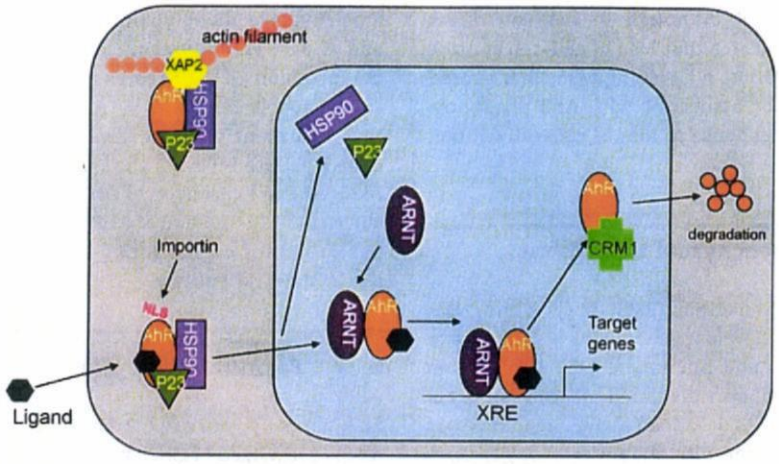

Fig. 1 – Regulation of AhR localization. In cytosol, AhR is complexed with hsp90, p23, and XAP2 (the last of which anchors the ligand-free receptor to the cytoskelton). Ligand binding results in AhR nuclear transport mediated by importins and is followed by dimerization with aryl hydrocarbon nuclear translocator (ARNT). The AhR/ARNT complex binds to xenobiotic responsive element (XRE), and induces transcription of target genes. AhR protein is exported by chromosome region maintenance 1 (CRM1), followed by degradation in cytosol.

these serine residues are phosphorylated to be anchored in cytoplasm under confluent culture. Using immunoblotting analysis, it was also shown that the relative amount of AhR in the nucleus was gradually decreased in proportion to the cell density. These observations led us to examine whether altered intracellular localization of AhR reflects AhR/ARNT-mediated transcription. Reporter analysis using luciferase cDNA connected to the XRE sequence, revealed that AhR activity was also affected by cell density. While the maximal luciferase activity was observed in subconfluent culture, the luciferase activity decreased to the basal level in confluent culture. These observations showed that subcellular localization and transcriptional activity of AhR were regulated by cell density.

Cell density dependent regulation system is reminiscent of contact inhibition. Cell growth is regulated by cell–cell contact in non-transformed cells. When cultured cells are maintained in low density, cells are actively growing. When cells grow to form confluent monolayer, they stop dividing. Critical anti-proliferative signals are mediated by cell–cell contact. It is very interesting to postulate that AhR is involved in regulation of contact inhibition. Recently, Weiss et al. indicated that TCDD treatment in WB-F344 rat liver cells leads to induction of JunD, resulting in up-regulation of cyclinA which triggers a release from contact inhibition via the AhR [39]. While exposure of confluent cells to TCDD-induced further proliferation, subconfluent cells did not respond to TCDD, suggesting that TCDD treatment specifically interferes with the signaling cascade of contact inhibition. It is suggested that this TCDD effect is an AhR-dependent and ARNT-independent reaction since suppression of AhR expression by siRNA abrogates the TCDD effect in sharp contrast with the suppressed expression of ARNT.

Previous reports showed that localization and transcription activity of AhR were altered in several cell lines when cell–cell contact was disrupted [11–13]. Recently, Cho et al. reported that suspension culture of C3H10T1/2 fibroblasts in methylcellulose-containing semisolid media resulted in activation of AhR-mediated transcription [40]. The AhR antagonist α-naphthoflavone blocked ligand-stimulated AhR activity, but did not affect the suspension-induced activation of AhR-mediated transcription, implying that the mechanism of the latter is different from that of former. They found that the activation of AhR by ligands can be clearly distinguished from the activation of AhR by the loss of cellular contact. We have shown that AhR is activated in the cells at the wounded edge in *in vitro* wound healing analysis using green fluorescent protein as a reporter of transcriptional activation by AhR/ARNT complex [36], suggesting that the loss of cell–cell contact leads to AhR activation. Owens et al. indicated the importance of Src family kinases in the disruption of cadherin-dependent cell–cell contact [41]. Src kinase is known to be associated with AhR complex [42]. Ligand binding to the AhR causes Src kinase to dissociate from the AhR complex and translocate from cytoplasm to the membrane [43], thereby increasing its own kinase activity which may be required for promoting destabilization of cell–cell contact. They showed that inhibition of the catalytic activity of the Src kinase stabilizes cadherin-dependent cell contacts, suggesting that Src kinase activity is required to disassemble cell–cell contacts. On the other hand, the Src kinase activity stimulates the epidermal growth factor receptor (EGFR) [44] which is known to play an important role in activation of MAPK pathways and other key signal transduction cascades. Activation of MAPK pathways promotes downstream signaling such as ERK and p38. Our results suggested that loss of cell–cell contact generates signals that increase the phosphorylation level of AhR (i.e., phosphorylation of Ser-68 which is located in the NES), thereby causing AhR to accumulate in the nucleus owing to inhibition of the

Please cite this article in press as: Ikuta T, et al. AhR protein trafficking and function in the skin. Biochem Pharmacol (2008), doi:10.1016/j.bcp.2008.10.003

export activity. It is likely that activated p38 MAPK is involved in this phosphorylation [36]. Although to date no direct experimental evidence indicates that loss of cell–cell contact is the signal for AhR activation, a signaling cascade triggered by Src kinase appears to be associated with AhR phosphorylation and activation in response to loss of cell–cell contact (Fig. 2).

4. Epithelial–mesenchymal transitions

Epithelial–mesenchymal transitions (EMT) occur during critical phases of embryonic development [45] as well as tumor progression to the metastatic phenotype [46]. During this process, disruption of E-cadherin-mediated cell–cell contact is considered to be a key step. As described above, we found that the AhR activation is associated with disruption of cell contact in keratinocyte. This observation prompted us to examine whether AhR is involved in the regulation of EMT. In many types of cancer, the loss of E-cadherin expression is due to transcriptional repression [47,48]. Transcription factors including a family of zinc finger proteins of the Slug/Snail family are implicated in such repression [49–51]. We have shown that AhR participates directly as a transcription factor in the induction of Slug expression in the context of loss of cell–cell contact, which, in turn, regulates EMT [52]. The induced Slug was associated with reduced level of the epithelial marker, cytokeratin 18 and with increased level of the mesenchymal marker, fibronectin. Belguise et al. [53] investigated the control of EMT in breast cancer. Ectopic coexpression of CK2 and NFκB c-Rel in untransformed mammary epithelial cells was sufficient to induce a mesenchymal invasive phenotype, in association with induction of AhR and Slug. The up-regulation of Slug was abrogated by coexpression of AhR repressor (AhRR), indicating that Slug expression is regulated by AhR. Furthermore, they showed that treatment with the green tea polyphenol epigallocatechin-3 gallate reversed the malignant phenotype as well as reduced the expression of AhR and Slug. Thus, these results suggest that activation of AhR signaling and induction of Slug are important events during the process of progression into the invasive phenotype.

5. Formation of epidermal tissue

Skin acts as a defense barrier against environmental stimuli and is composed of two layers, the dermis and epidermis. The epidermis is divided into several layers and extends from the basement membrane to the outer surface. The basal layer contains the basal keratinocytes where mitosis occurs. As the keratinocytes mature, they form the spinous layer, granular layer, and stratum corneum which has the barrier function (Fig. 3A). Keratinocytes in the spinous and the granular layer produce differentiation-specific proteins including filaggrin and loricrin which are cross-linked by transglutaminase into cornified envelopes [54].

Fernandez-Salguero et al. [55] investigated skin lesions in AhR-null mice and found an association of structurally abnormal hair fibers, rupture of hair follicles and mixed inflammatory cells infiltrate that progressed to acute ulcers. It has been reported that TCDD affects differentiation of

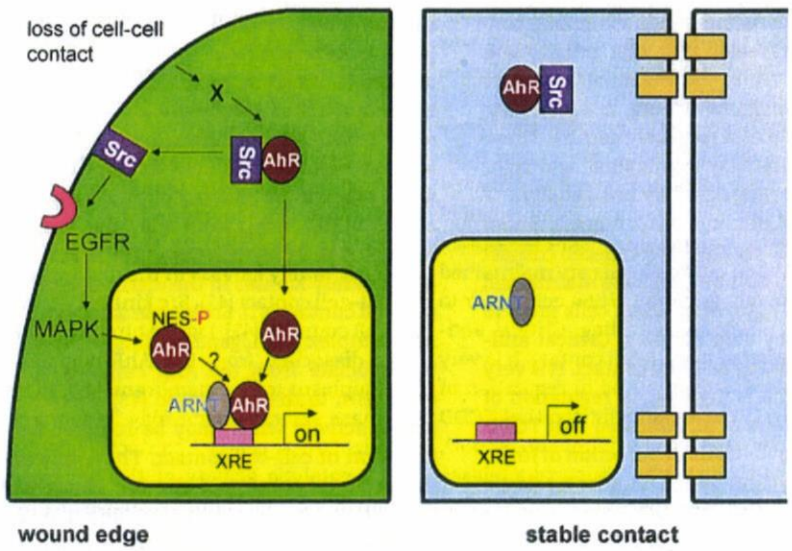

Fig. 2 – A model for AhR localization controlled by cell–cell contact in the *in vitro* wound healing assay. Stable contact (right) mediated by adhesion molecules such as E-cadherin is mechanically disrupted to form wound edge (left). The unknown signal (X) triggered by the loss of cell–cell contact activates AhR, resulting in dissociation of Src from the AhR complex and translocation from the cytosol to the membrane, where its kinase activity required for disruption of cell–cell contact is activated. In addition, Src kinase activity may act as a trigger for the signals such as epidermal growth factor receptor (EGFR)-dependent pathway that induces key signal transduction cascades including MAPK. It is likely that activated p38 MAPK is involved in the phosphorylation of the nuclear export signal (NES) of AhR, which in turn inhibits nuclear export resulting in nuclear accumulation. XRE-mediated transcription is up-regulated by AhR/ARNT complex.

Please cite this article in press as: Ikuta T, et al. AhR protein trafficking and function in the skin. Biochem Pharmacol (2008), doi:10.1016/j.bcp.2008.10.003

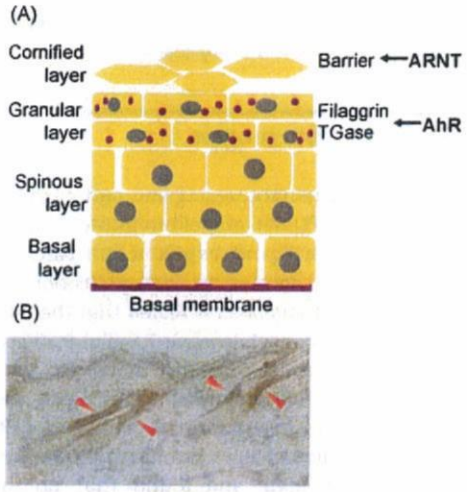

Fig. 3 – (A) Structure of the epidermis, and the possible role of AhR and ARNT. AhR stimulates the expression of filaggrin and transglutaminase 1 (TGase) in granular cells. Barrier formation requires expression of ARNT. (B) Immunohistochemistry for AhR localization on the back skin from 3-wk-old WT C57Bl mice. After excision, the tissue was embedded in O.C.T. compound (Miles, Elkhart, IN) and immediately frozen using liquid carbon dioxide. Frozen tissue was sectioned at 8 μm intervals, and the sections were fixed by 4% formaldehyde before overnight incubation with anti-AhR antibody (BIOMOL, Plymouth Meeting, PA) at 4 °C. Arrowheads indicate the site of immunoreactivity including upper part of hair follicle.

keratinocytes. Loetscher et al. [56] examined the effects of TCDD on developing skin of the C57Bl/6J mouse strain. Examination of mouse fetal skin at embryonic day (E) 16 revealed that expression of filaggrin is accelerated in individuals exposed *in utero* to TCDD at E13. They reported that the two putative XREs are present upstream of the transcription start site of human profilaggrin gene. In addition, Du et al. [57] studied the effect of TCDD on differentiation program of human epidermal keratinocytes and showed the induction of transglutaminase 1 at the mRNA and protein levels. This was further confirmed by the increasing transglutaminase 1-mediated cross-linking activity *in situ*. Since there is no XRE motif in the human transglutaminase 1 promoter region, it is unclear how TCDD regulates transglutaminase 1 expression. These investigations suggest that AhR has roles in the modulation of differentiation of keratinocytes.

The function of the skin barrier is partly dependent on terminal differentiation of keratinocytes. The cells differentiate as they move to the skin surface. The stratum corneum is composed of not only insoluble protein such as involucrine and filaggrin but also lipid complex containing cholesterol, ceramides, and fatty acids. Takagi et al. [58] and Geng et al. [59] reported defects in the barrier function in ARNT-deficient mice. They showed that defects in lipid metabolism resulted in failure of the epidermal barrier function. ARNT-disrupted newborn mice died neonatally of severe dehydration caused by water loss. We are interested to investigate whether AhR is involved in these processes as a heterodimer-partner of ARNT although AhR-null mice have not yet been reported to show such a severe skin phenotype.

To elucidate the AhR function in skin, we examined AhR localization in murine skin by immunohistochemistry. One of the regions in which AhR was detected is the upper part of the hair follicle including the infundibulum (Fig. 3B). Exposure of mammals to TCDD produces an array of pathological manifestations including teratogenesis [3], hepatotoxicity [4], and dermatopathology [60]. Chlorance, a hyperkeratotic skin disorder, is a specific type of acne-like skin disease affecting the hair follicle and inter follicular epidermis and has been used as a hallmark of TCDD exposure in humans. Histopathological analysis of the skin with chloracne has revealed acne-like appearance with hyperkeratosis. In severe cases of acne, the rupture of the infundibulum is associated with inflammation. It is reported that transgenic mice expressing a constitutively active form of AhR in keratinocytes develop severe skin lesions accompanied by inflammation resembling typical atopic dermatitis with increased expression of inflammation-related genes (such as the genes for interleukins and chemokines) [61]. When infundibula maintained in culture were stimulated with interleukin-1α, hyperkeratosis that was similar to that seen in acne was observed [62]. Taken together, these results prompted us to consider that in response to TCDD exposure, AhR expressed in infundibula is aberrantly activated to induce hyperplasia and inflammation, resulting in chloracne.

6. AhR functions in skin wound healing

Skin wound healing is a dynamic three-phase process: inflammation, tissue formation, and tissue remodeling [16]. Diverse cell types including leukocytes, keratinocytes and dermal fibroblasts participate in each phase. For example, in the early phase of healing, inflammatory leukocytes are recruited to the wounded site. Neutrophils cleanse the wound area of foreign particles, and macrophages release cytokines and growth factors. Keratinocytes migrate and proliferate to cover the wound area, and the dermal fibroblasts synthesize extracellular matrix for tissue remodeling. It is reported that AhR is expressed in these cells [40,63–65]. Here, we investigated the role of AhR in skin wound healing using either wild-type mice, mice heterozygously or homozygously deficient for the AhR gene.

Our methods of full thickness dorsal skin wounding damaged both the epidermis and the underlying dermis. All mice were 8–10 wk old, anesthetized, and received a single 5-mm-diameter excisional wound on the shaved mid-dorsal skin. Mice were kept separately in cages to prevent fighting. Wound closure was determined and expressed as a percentage of the total surface of the wound (Fig. 4). The wounds closed almost completely at day 12 irrespective of AhR genotype. However, in the early phase of healing, wound area decreased faster in the AhR−/− mice than in the wild-type mice and AhR± mice. The time needed for 50% closure in wild-type, AhR± and AhR−/− mice was 73.7 ± 3.0 h ($n = 50$), 59.0 ± 3.3 h ($n = 32$) and 47.6 ± 3.3 h ($n = 39$), respectively. The difference in time needed for 50% closure between AhR−/−

Please cite this article in press as: Ikuta T, et al. AhR protein trafficking and function in the skin. Biochem Pharmacol (2008), doi:10.1016/j.bcp.2008.10.003

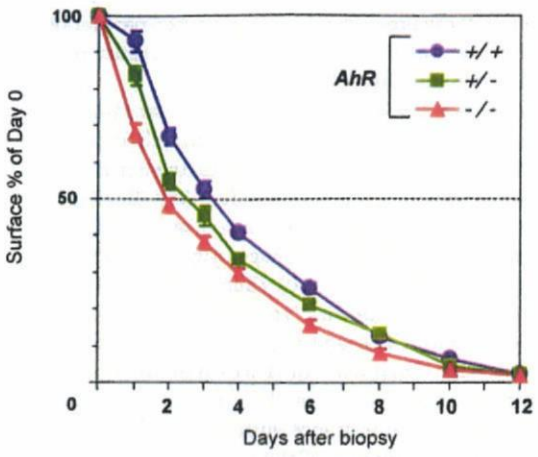

Fig. 4 – Surface areas of the wounds. The back skin of each mouse (8–10 wk) was shaved 1 wk before wounding. A full thickness of mid-dorsal wound (5 mm in diameter) was created and the wound areas were quantified on the indicated days until complete healing, using NIH image software. The surfaces are plotted as percentage of the surface of the wound at day 0 (Mean ± SE). The surface areas of the wounds at day 0 were not significantly different among genotypes.

and wild-type mice was significant ($P = 1.97E-08$). On the other hand, we did not find any differences in repair processes between wild-type and AhRR−/− mice. These data suggest that inactivation of AhR accelerates wound closure during the early phase, which corresponds to the inflammatory phase, of wound healing. These observations are reminiscent of those observed for peroxisome proliferator-activated receptor (PPAR)-mutant mice. Michalik et al. [66] found that wound healing in PPARα−/− mice was delayed during the first 4 days after injury, suggesting the involvement of inflammation. They further assessed inflammatory infiltration by counting neutrophils and monocytes/macrophages present in the wound bed. Recruitment of neutrophils and monocytes was impaired in the PPARα−/− mice at day 1. AhR expression has been detected in monocytes and macrophages [63,64] and might affect the function of these cells. Tauchi et al. [61] reported that transgenic mice expressing the constitutive active form of AhR in keratinocytes develop severe skin lesions accompanied by inflammation. It is likely that the skin of AhR−/− mice has a reduced inflammatory phenotype. Aschcroft et al. [67] investigated the role of Smad3, a mediator of TGF-β signaling, in skin wound healing. They reported that mice lacking Smad3 show accelerated wound healing accompanied by reduced inflammatory response (i.e., reduced local infiltration of monocytes) leading to reduced level of TGF-β in the wound site. One possible explanation for the increased rate of re-epithelialization in mice lacking Smad3 is the increase in keratinocyte proliferation due to abrogation of the growth inhibitory effect of TGF-β. In our experiments, we attribute this phenomenon (i.e., faster decrease in wound area in AhR-deficient mice in the early phase of wound healing) to reduced inflammation. In wild-type mice, AhR may play a supportive role in the inflammatory response.

7. AhR in skin carcinogenesis

AhR is considered to mediate teratogenic and carcinogenic effects. Benzo[a]pyrene (B[a]P), one of environmental chemicals binding to AhR as a ligand, exerts potent carcinogenic activity in several animal species. Topical application of B[a]P produces skin tumors. It has been revealed that the ultimate metabolite of B[a]P (i.e., benzo[a]pyrene-7,8-diol-9,10-epoxide [BPDE], which is synthesized in the metabolic pathway involving cytochrome P450 isoforms) forms DNA adducts and acts as a mutagen. To investigate the contribution of AhR to carcinogenesis, Shimizu et al. [2] examined the response of AhR-deficient mice to B[a]P and found that no tumors appeared in the AhR-deficient mice. They provided direct evidence that AhR is required for skin tumor induction by benzo[a]pyrene.

An important problem in skin cancer research is the identification of the target cells for chemical carcinogenesis. Evidence is accumulating that a subpopulation known as stem cells are the targets of carcinogenesis [68–70]. A number of investigations revealed that initiated cells persist in the epidermis essentially for the life of the animal, suggesting that the initiated cells are not simply proliferating cells but also stem cells. Morris et al. [15] examined the origin of skin tumors. They completely removed the interfollicular epidermis of carcinogen-initiated mice using an abrasion technique although the hair follicles remained undisturbed. The interfollicular epidermis after abrasion regenerated from cells in the hair follicles. Subsequently, tumor promotion was progressing. Although mice with abraded skin developed papillomas and carcinomas, the number of papillomas was half that of mice with unabraded skin. These results suggest that target of tumor initiation is the cells in hair follicles and, to a lesser degree, in the interfollicular epidermis.

One of the cell surface markers of hair follicle stem cells is CD34. Trempus et al. [68] examined whether CD34 participates in two-stage skin carcinogenesis in CD34 knockout (KO) mice since hair follicle stem cells are thought to be a major target of carcinogens. CD34KO mice failed to develop papillomas, suggesting the requirement of stem cells for skin tumor development. Hair follicle stem cells may be a target for carcinogens. If so, stem cell may express AhR to induce P450 isoforms that metabolically activate carcinogens. It has been shown that hematopoietic stem cells, which express functional AhR, have been shown to be a target of polycyclic aromatic hydrocarbons [71]. Treatment of these cells with B[a]P resulted in impairment of cell expansion and inhibition of cell differentiation into various cell lineages including erythrocyte, granulocyte, macrophage, and megakaryocyte. These toxic effects are related to P450-dependent B[a]P metabolite formation. These results suggest that AhR is functional in the system in stem cells.

Thus, it is implied that stem cells are critical targets of carcinogen metabolites produced by P450 isoforms. These metabolites may be involved in the initiation of the stem cell in

Please cite this article in press as: Ikuta T, et al. AhR protein trafficking and function in the skin. Biochem Pharmacol (2008), doi:10.1016/j.bcp.2008.10.003

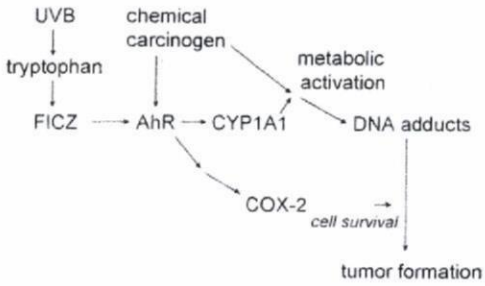

Fig. 5 – Roles of AhR in skin carcinogenesis. CYP1A1 is induced by chemical carcinogens as well as photoproducts of tryptophan [72,73] such as 6-formylindolo[3,2-b]carbazole (FICZ) generated intracellularly by UVB exposure. DNA adducts are formed by reaction with metabolically activated carcinogens. FICZ also induces COX-2 expression through EGFR activation. The COX-2 pathways promote cell survival, resulting in the tumor formation. AhR directly induces CYP1A1 which stimulates generation of initiated cells, and indirectly induces expression of COX-2 leading to tumor promotion.

skin carcinogenesis resulting in the proliferation of the initiated stem cells.

Another risk for skin carcinogenesis is ultraviolet radiation. Photoproducts of tryptophan are known to have high affinity for AhR and are postulated as endogenous ligands [72,73]. The UVB portion (280–315 nm) of the spectrum is a principal risk factor for skin cancer. Fritsche et al. [44] found intracellular formation of the AhR ligand 6-formylindolo[3,2-b]carbazole (FICZ) after UVB irradiation of murine skin and human keratinocyte cell line. AhR activation induces *CYP1A1* gene expression and EGFR internalization and subsequent induction of cyclooxygenase-2 (*COX-2*) gene expression. COX-1 and COX-2 catalyze the first reaction in the conversion of arachidonic acid to prostaglandins. Prostaglandin E_2 is the major product found in UV-exposed skin. In most tissues, COX-1 is constitutively expressed, whereas COX-2 is highly inducible by a variety of inflammatory and tumor-promoting stimuli [74] and is constitutively up-regulated in skin carcinomas [75]. To understand the contribution of COX-1 and COX-2 to UV-carcinogenesis, Fischer et al. [76] performed UV-induced-carcinogenesis experiments using wild-type mice and mice heterogeneously for the COX-1 or the COX-2 gene. While the tumor generations of COX-1± mice and COX-1+/+ mice were essentially similar, the tumor multiplicity in COX-2± mice was reduced to 50–65% and the tumor size was markedly decreased compared with that of wild-type mice. Studies have revealed that UV-induced COX-2 expression contributes to the acquisition of resistance to epidermal apoptosis [77].

In conclusion, UVB exposure induces CYP1A1 and COX-2 in keratinocytes. In this intracellular environment, active carcinogens produced by CYP1A1 may form DNA adducts resulting in generation of initiated cells. Furthermore, as a result of acquiring resistance to apoptosis by induction of COX-2, the initiated cells may be able to clonally expand into detectable skin tumors (Fig. 5).

8. Perspective

Current investigations have revealed that AhR is an important regulator in various tissues even in the absence of exogenous ligands. While identification of endogenous ligands of AhR is one of the most intriguing goals of future study, uncovering the signaling pathway leading to AhR activation in the context of cell–cell contact is also needed. Investigating target genes of AhR/ARNT is also important for elucidation of AhR function. In wound healing, we are interested in the genes that act downstream of AhR in the signaling pathway and are involved in inflammatory agent production such as the release of cytokines. In skin carcinogenesis by benzo[a]pyrene, AhR is believed to be necessary for the induction of CYP1A1 which yields active carcinogens. However, the experimental data indicating that AhR-deficient mice produce no tumors do not exclude the possibility that AhR is involved in cancer progression. It would also be interesting to determine whether induction of epithelial–mesenchymal transitions mediated by AhR is functional in cancer.

Acknowledgements

This study was supported by the Grants-in-Aid for Scientific Research from the Japanese Ministry of Education, Culture, Sports, Science and Technology.

REFERENCES

[1] Abbott BD, Birnbaum LS, Perdew GH. Developmental expression of two members of a new class of transcription factors: I. Expression of aryl hydrocarbon receptor in the C57BL/6N mouse embryo. Dev Dyn 1995;204:133–43.
[2] Shimizu Y, Nakatsuru Y, Ichinose M, Takahashi Y, Kume H, Mimura J, et al. Benzo[a]pyrene carcinogenicity is lost in mice lacking the aryl hydrocarbon receptor. Proc Natl Acad Sci 2000;97:779–82.
[3] Mimura J, Yamashita K, Nakamura K, Morita M, Takagi TN, Nakao. et al. Loss of teratogenic response to 2,3,7,8-tetrachlorodibenzo-*p*-dioxin (TCDD) in mice lacking the Ah (dioxin) receptor. Genes Cells 1997;2:645–54.
[4] Walisser JA, Glover E, Pande K, Liss AL, Bradfield CA. Aryl hydrocarbon receptor-dependent liver development and hepatotoxicity are mediated by different cell types. Proc Natl Acad Sci 2005;102:17858–63.
[5] Quintana FJ, Basso AS, Iglesias AH, Korn T, Farez MF, Bettelli E, et al. Control of T(reg) and T(H)17 cell differentiation by the aryl hydrocarbon receptor. Nature 2008;453:65–71.
[6] Veldhoen M, Hirota K, Westendorf AM, Buer J, Dumoutier L, Renauld JC, et al. The aryl hydrocarbon receptor links TH17-cell-mediated autoimmunity to environmental toxins. Nature 2008;453:106–9.
[7] Baba T, Shima Y, Mimura J, Oshima M, Fujii-Kuriyama Y, Morohashi KI. Disruption of aryl hydrocarbon receptor (AhR) induces regression of the seminal vesicle in aged male mice. Sex Dev 2008;2:1–11.
[8] Baba T, Mimura J, Nakamura N, Harada N, Yamamoto M, Morohashi K, et al. Intrinsic function of the aryl hydrocarbon (dioxin) receptor as a key factor in female reproduction. Mol Cell Biol 2005;25:10040–51.

Please cite this article in press as: Ikuta T, et al. AhR protein trafficking and function in the skin. Biochem Pharmacol (2008), doi:10.1016/j.bcp.2008.10.003